# Theory of the magnetic-field-induced metal-insulator transition

Jin An,[1,2] C. D. Gong,[3] and H. Q. Lin[2,*]
[1]*National Laboratory of Solid State Microstructures, Nanjing University, Nanjing 210093, China*
[2]*Department of Physics, The Chinese University of Hong Kong, Hong Kong*
[3]*Chinese Center of Advanced Science and Technology (World Laboratory), P.O. Box 8730, Beijing 100080, China*
(Received 26 April 2000; revised manuscript received 13 November 2000; published 12 April 2001)

We study the properties of electronic systems in the presence of a magnetic field. For the quasi-one-dimensional chain, the magnetic-field-induced metal-insulator transitions are investigated with uniform and nonuniform magnetic flux, respectively. For the two-dimensional square lattice, metal-insulator transitions can be achieved at both zero and nonzero temperatures when staggered magnetic flux is turned on. Moreover, a pesudogap is opened on the two-dimensional square Fermi surface. When we introduce fluctuations into the perfect staggered magnetic field and increase its magnitude, a finite region of the Fermi surface around $(\pi/2,\pi/2)$ would be gradually formed with decreasing bandwidth. For both one- and two-dimensional cases, the temperature and flux dependence of the induced currents are obtained and it is shown that the current state with staggered flux distribution in two dimensions is stable.

DOI: 10.1103/PhysRevB.63.174434 PACS number(s): 71.30.+h, 71.10.Fd

## I. INTRODUCTION

Since the discovery of the quantum Hall effect[1,2] and colossal magnetoresistance,[3,4] quantum systems under an external field have attracted much attention recently.[5–11] Among many characteristic properties, the field-induced phase transition in these systems is particularly interesting to both theoreticians and experimentists. According to the scaling theory of localization, all states in a two-dimensional system are localized. Some early studies agreed with this conclusion.[12–16] However, in the presence of a magnetic field, extended states can appear due to the broken time-reversal symmetry, as shown for the quantum Hall system.[1,2] Theoretically, a magnetic-field-induced metal-insulator transition due to a random magnetic field in a two-dimensional noninteracting electronic system has been confirmed by several groups.[5–8] They have argued that in the presence of a random magnetic field the states in the center of the band are delocalized and the density of states exhibits singularity. Experimentally, metal-insulator transitions have been observed in two-dimensional electron systems in silicon.[9,10] There has also been a report on the metal-insulator transition in the presence of spin-orbit coupling in two-dimensional systems.[11] Furthermore, Ugajin found a sharp electric-field-induced metal-insulator transition in a two-dimensional two-layered system.[17] The apparent conflict between these experiments and the scaling theory of localization has been resolved recently by formulating the scaling theory in the presence of electron-electron interactions.[18] However, it is not clear what would happen on the metal-insulator transition when the interaction between electrons and the magnetic field are both present. This is the issue we want to resolve. More recently, the electronic transmission properties with inhomogeneous flux in quasi-one-dimensional chains have been studied numerically and show very interesting transmission behavior which might be useful in the application to fabricate special devices.[19–21] In fact, it is now experimentally possible to construct and detect the inhomogeneous field at the scale of deep sub-$\mu$m and thus the properties of quantum systems under a magnetic field are also very attractive and essential to experimentalists.

In this paper, we have investigated from a different view the magnetic-field-induced metal-insulator transition in quasi-one- and two-dimensional systems where the loops formed by the electron hopping paths are threaded by magnetic flux. The systems are somewhat different from those studied before. Particularly in the two-dimensional case, we have used the Hubbard model to study the interacting electron system with the Hartree-Fock approximation. A field-induced pseudogap behavior was found to appear.

These systems we have studied are something like perfect networks of Aharonov-Bohm (AB) rings.[22] So we also study the AB effect and the induced current distributions in these systems. Under the effect of an external magnetic field the waves describing the currents propagating from left to right, along two branches of the ring (the AB ring), suffer a phase shift. Because of the phase shift there is a constructive or destructive interference, reflected in the conductance as a periodic function with period $\phi_0 = hc/e$.

The paper is organized as follows. In the next section, quasi-one-dimensional chains are discussed by using the tight-binding model as an illustration, for all the states would be localized and so there is no metal-insulator transition at all if any interaction between particles or disorder are considered.[23,24] We will first introduce uniform magnetic flux and study the one-band and the two-band cases, respectively. Second, nonuniform magnetic flux is introduced and the one-band case is considered. In Sec. III, we investigate the two-dimensional square lattice with a staggered magnetic flux. In addition we also study effects of electron-electron correlation by using the Hubbard model. Disorder effects are also studied in this section. We summarize our conclusions in Sec. IV.

## II. QUASI-ONE-DIMENSIONAL CASE

In this section, we study a quasi-one-dimensional system with lattice structure as shown in Fig. 1. Each lattice site is

 

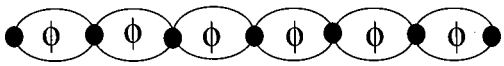


FIG. 1. A quasi-one-dimensional chain with sites connected to each other by two hopping paths. Each loop is threaded by a uniform magnetic flux $\phi$.

connected to its nearest neighbor by a loop which is threaded by a uniform magnetic flux $\phi$. If $\phi=0$, the system is just described by the usual tight-binding model with the following Hamiltonian:

$$H=\sum_{i,\alpha}\ \epsilon_\alpha c_{i\alpha}^{+}c_{i\alpha}-2\sum_{i\alpha\alpha'}\ (t_{\alpha\alpha'}c_{i+1\alpha'}^{+}c_{i\alpha}+\text{H.c.}), \quad (1)$$

where $\alpha$ denotes the energy level and $\epsilon_\alpha$ represents the site energy of the system, respectively. Here, we omit spin indices for simplicity. Hopping integrals $t_{\alpha\alpha'}$ are real quantities for $\phi$ equal to zero. However, if $\phi$ is nonzero, electrons propagating along the upper and lower paths of the chain would acquire a different phase shift and that would induce an interference between them, due to the Aharonov-Bohm effect.[22] This means that the hopping integrals will be modulated by the external magnetic field through a field-dependent phase factor:

$$2t\rightarrow te^{i\delta/2}+te^{-i\delta/2}=2t\cos\delta/2, \quad (2)$$

where $\delta=2\pi\phi/\phi_0$ and $\phi_0=hc/e$ is the magnetic-flux quanta.

First, let us investigate the single-band case at half filling. The energy spectrum is then

$$\epsilon_k=-4t\cos(\delta/2)\cos ka, \quad (3)$$

and the bandwidth is $W=8t|\cos\delta/2|$. It is obvious that $W$ is a periodic function of $\phi$ with period $\phi_0$, although the energy spectrum $\epsilon_k$ is a function with period $2\phi_0$, not $\phi_0$, for $\epsilon_k$ changes sign when $\phi=\phi_0$. In fact, the characteristic of period $2\phi_0$ could not be detected in experiments, because the Fermi levels corresponding to the two cases are identical, and the majority of thermodynamic quantities depend mostly only on physical properties of electrons near the Fermi level. In the following discussion, we shall show that the transport properties (for example, current and conductance) are also periodic functions of $\phi$ with period $\phi_0$.

With the energy spectrum given by Eq. (3), let us calculate the current of each channel in the system without applying external electric field. Accordingly, the ''left'' and ''right'' symmetry is held so the current could occur only in the form resembling the persistent current[25,26] found in mesoscopic rings. Let ''+'' and ''−'' denote the current flowing in the upper and lower channels, respectively, one has

$$I_{(\pm)}=\frac{e}{\hbar}(te^{\pm i\delta/2}\langle c_{i+1}^{+}c_i\rangle-\text{H.c.}). \quad (4)$$

After simple manipulations, the following expressions for the current can be obtained:

$$I_{(\pm)}=\frac{2et}{N\hbar}\sum_k\ \sin(ka\pm\delta/2)f_F(\epsilon_k), \quad (5)$$

where $f_F(\epsilon_k)=1/(1+e^{\beta(\epsilon_k-\epsilon)})$ and $N$ is the total number of lattice sites. From Eq. (5), it can be seen that $I_{(+)}=-I_{(-)}$, which is nothing but the condition for a circulating persistent current in a ring. At zero temperature, one gets

$$I_{(+)}=\text{sgn}(\pi-\delta)\frac{4et}{h}\sin(\delta/2)\ \ (0<\delta<\pi). \quad (6)$$

Note that when $\phi$ is modulated through the value $\phi=\frac{1}{2}\phi_0$, the current changes direction abruptly. This is attributed to the exchange between the top and the bottom of the energy band.

Next we turn on the electric field $E$ and discuss its influence on the conductance. According to the Boltzmann transport equation, one obtains the deviation of the momentum distribution of electrons $\delta n_k$ from its equilibrium value $n_k^0=f_F(\epsilon_k)$,

$$\delta n_k=-eE\tau(k)\frac{\partial n_k^0}{\partial(\hbar k)}, \quad (7)$$

where $\tau(k)$ is the relaxation time at momentum $k$ which should be independent of $\phi$ and can be determined by considering the detailed scattering process.[27] Combining Eqs. (6) and (7), one can obtain an additional field-dependent part of the current at zero temperature:

$$\delta I_{(+)}=\frac{2eat}{h}2\frac{eE}{\hbar}\tau(k_F)|\cos\delta/2|$$

$$=\frac{4e^2a}{h}\frac{Et}{\hbar}\tau(k_F)|\cos\delta/2|=\delta I_{(-)}. \quad (8)$$

Then one gets the total induced current $\delta I=\delta I_{(+)}+\delta I_{(-)}=2\delta I_{(+)}$ and the conductance

$$\sigma=\frac{2e^2}{h}\frac{2\tau(k_F)t}{N\hbar}|\cos\delta/2|=\frac{2e^2}{h}\frac{2\tau(k_F)t}{N\hbar}\frac{W}{8t}. \quad (9)$$

Again, the conductance is a periodic function of $\phi$ with period $\phi_0$. Also the conductance is proportional to the bandwidth $W$. Since $W$ can be modulated continuously from 0 to $8t$, the conductance also changes from zero to a finite value. Thus the system could undergo a metal-insulator transition *continuously*.

Second, let us consider the situation with two levels per site, i.e., the two-band case, described by the following model Hamiltonian in $k$ space:

$$H=\sum_k\ (\epsilon_{k\alpha}c_k^{+}c_k+\epsilon_{k\beta}d_k^{+}d_k)+\sum_k\ \gamma_k(d_k^{+}c_k+\text{H.c.}), \quad (10)$$

where $\alpha$ and $\beta$ refer to the two energy levels, $c_k$ and $d_k$ are corresponding annihilation operators, and other parameters are

$$\epsilon_{k\alpha}=\epsilon_\alpha-4t_{\alpha\alpha}\cos\delta/2\cos\kappa a,$$

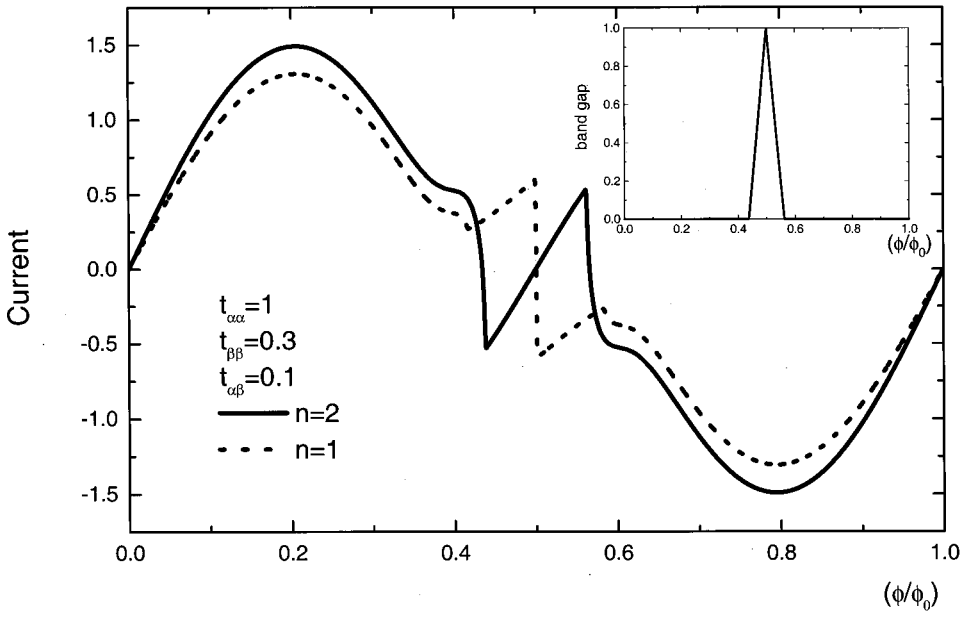


FIG. 2. Induced current versus magnetic flux $\phi/\phi_0$ for the two-band case at half filling (solid line) and full filling (dotted line). Parameters are: $\epsilon_\alpha-\epsilon_\beta=1$, $t_{\alpha\alpha}=1$, $t_{\beta\beta}=0.3$, $t_{\alpha\beta}=0.1$. Inset: band gap versus the magnetic flux.

$$\epsilon_{k\beta}=\epsilon_\beta-4t_{\beta\beta}\cos\delta/2\cos ka,$$

$$\gamma_k=4t_{\alpha\beta}\cos\delta/2\cos ka, \tag{11}$$

with $\epsilon_\alpha$ and $\epsilon_\beta$ being the site energies, $t_{\alpha\alpha}$ and $t_{\beta\beta}$ intraband hopping transfers, and $t_{\alpha\beta}$ interband transfers. The energy spectrum is

$$\epsilon_k^{\pm}=\frac{1}{2}\{(\epsilon_{k\alpha}+\epsilon_{k\beta})\pm\sqrt{(\epsilon_{k\alpha}-\epsilon_{k\beta})^2+\gamma_k^2}\}. \tag{12}$$

The total current in the absence of external electric field for each channel is the sum of the intraband and interband currents,

$$I_{(+)}=\frac{e}{\hbar}[e^{i\delta/2}(t_{\alpha\alpha}\langle c_{i+1}^+c_i\rangle+t_{\beta\beta}\langle d_{i+1}^+d_i\rangle+t_{\alpha\beta}\langle c_{i+1}^+d_i\rangle+t_{\alpha\beta}\langle d_{i+1}^+c_i\rangle)-\text{H.c.}]=-I_{(-)}. \tag{13}$$

These expectations can be calculated exactly and we obtain the following result for the current:

$$I_{(+)}=\frac{e}{\hbar}\sin\delta/2\sum_k\cos ka\{f(\epsilon_k^+)[t_{\alpha\alpha}(\epsilon_k^+-\epsilon_{\beta k})+t_{\beta\beta}(\epsilon_k^+-\epsilon_{\alpha k})-2t_{\alpha\beta}\gamma_k]-f(\epsilon_k^-)\times[t_{\alpha\alpha}(\epsilon_k^--\epsilon_{\beta k})+t_{\beta\beta}(\epsilon_k^--\epsilon_{\alpha k})-2t_{\alpha\beta}\gamma_k]\}. \tag{14}$$

The flux dependence of the currents at half filling and full filling are shown in Fig. 2. It can be seen that at half filling, the direction of the current changes abruptly at $\phi_0/2$, similar to the uniform flux case discussed above. While at full filling, the current oscillates around $\phi_0/2$ and its direction changes four times in a period of $\phi$, which is quite unusual. This oscillation of the current comes from the competition between the intraband and interband currents, for they are opposite in directions.

Compared with the one-band case, there exists an energy gap for the two-band case and the band gap $\Delta=\epsilon_k^+(\min)-\epsilon_k^-(\max)$ is also a periodic function of $\phi$ with period $\phi_0$. What is important is that the band gap $\Delta$ could be modulated by the external magnetic field, by which many properties of the system (for example, electromagnetic absorption) could also be modulated by the magnetic field. Note that we expect a metal-insulator transition to occur at full filling by modulating $\phi$ if the parameters are so properly selected that the system is actually gapless in one region of $\phi$ and has a band gap in the other region (see the inset in Fig. 2). This is another type of magnetic-field-induced transition.

Finally we consider the one-band case with nonuniform magnetic flux, shown in Fig. 3, where the loops of the hopping channels are threaded by magnetic fluxes $\phi_1$ and $\phi_2$, alternatively. The energy spectrum is simply

$$\epsilon_k^{\pm}=\pm|\gamma_k|=\pm 2t\sqrt{\cos^2\delta_1/2+\cos^2\delta_2/2+2\cos\delta_1/2\cos\delta_2/2\cos 2ka}, \tag{15}$$

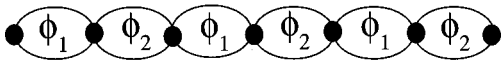


FIG. 3. A quasi-one-dimensional chain with sites connected to each other by two hopping paths. Each loop is threaded by an alternating magnetic flux $\phi_1$ and $\phi_2$.

where $\delta_i = 2\pi\phi_i/\phi_0$ $(i=1,2)$, and the band gap is

$$\Delta = 4t|\cos\delta_1/2 - \cos\delta_2/2|. \tag{16}$$

Equation (16) tells us that by adjusting magnetic fluxs $\phi_1$ and $\phi_2$ properly, the band gap $\Delta$ can be changed continuously from 0 to $8t$. For the half filled case, the lower subband is full filled completely while the upper subband is empty, so whether $\Delta$ is zero or not would affect drastically the conducting properties of the system. When the system is changed from the state of $\Delta=0$ to $\Delta\neq 0$, the effective lattice constant is also changed from $a$ to $2a$, and a Peierls-like metal-insulator transition occurs. This type of transition is different from the conventional Peierls transition[28,29] because there is no occurrence of lattice distortion. It is actually a magnetic-flux-induced metal-insulator transition.

### III. TWO-DIMENSIONAL CASE

For two dimensions, we study the Hubbard Hamiltonian defined on the square lattice,

$$H = -\sum_{\langle ij\rangle\sigma} t_{ij} c_{j\sigma}^{+} c_{i\sigma} + U\sum_i n_{i\sigma} n_{i\bar{\sigma}}, \tag{17}$$

where $\langle ij\rangle$ denotes nearest neighbors, $t_{ij}$ is the hopping integral, and $U$ is the Coulomb repulsion. We restrict ourselves to the half filled band case. For this particular case, it is quite clear that there exists long-range antiferromagnetic ordering for any nonzero $U$. Although the Hartree-Fock approximation usually overestimates symmetry breaking, it does give the correct answer for the half filled band case with small $U$, as validated by early analytical and numerical studies. The Hartree-Fock decoupling of the Hubbard interaction gives

$$n_{i\sigma}n_{i\bar{\sigma}} \simeq \langle n_{i\sigma}\rangle n_{i\bar{\sigma}} + n_{i\sigma}\langle n_{i\bar{\sigma}}\rangle - \langle n_{i\sigma}\rangle\langle n_{i\bar{\sigma}}\rangle. \tag{18}$$

Assuming long-range antiferromagnetic order, we have

$$\langle n_{i\sigma}\rangle = \frac{n}{2} + (-1)^i \sigma m, \tag{19}$$

where $n$ $(=1$ for the half filled band studied here) is the average number of electrons per site and $m$ is the antiferromagnetic order parameter defined by: $m = 1/2\langle (n_\uparrow - n_\downarrow)\rangle$. The mean-field Hamiltonian is given by (omitting the constant term)

$$H_{\mathrm{MF}} = \sum_{i\sigma}\left[\left(\frac{Un}{2} + mU\right)c_i^{+}c_i + \left(\frac{Un}{2} - mU\right)d_i^{+}d_i\right] - \sum_{\langle ij\rangle\sigma}(t_{ij}c_{j\sigma}^{+}d_{i\sigma} + t_{ij}^{*}d_{j\sigma}^{+}c_{i\sigma}), \tag{20}$$

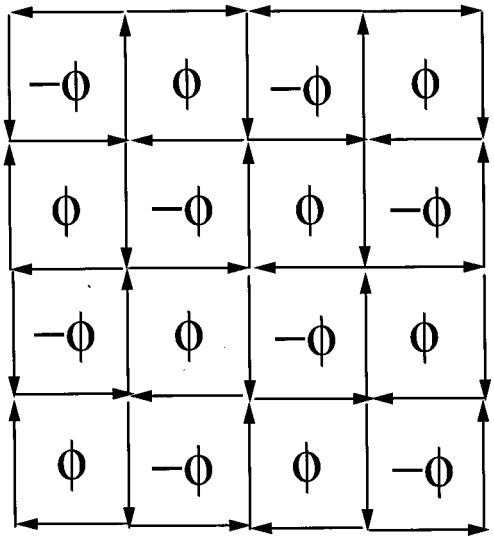


FIG. 4. A two-dimensional square lattice with plaquettes is threaded by alternative flux $\phi$ and $-\phi$. Electrons hopping along the arrows in the figure would suffer a phase shift $\delta/4$, where $\delta = 2\pi\phi/\phi_0$.

where we have divided the lattice into two sublattices with $c_i$ and $d_i$ the corresponding annihilation operators.

When staggered magnetic fluxes are introduced through the plaquette of the square lattice, as shown in Fig. 4, an interesting competing mechanism between the Coulomb repulsion and the staggered field would appear. The Coulomb repulsion $U$ tends to arrange nearest-neighbor spin pairs antiparallel, i.e., establishes antiferromagnetic ordering, while the staggered magnetic flux in each plaquette tends to turn the spins on the corners of the plaquette parallel to the direction of the flux, i.e., suppresses the antiferromagnetic order. Thus in the presence of the staggered magnetic flux, a critical value of Coulomb repulsion $U_c$ is needed in order to have the antiferromagnetic order.

As before, the hopping integral of electrons $t_{ij}$ should be modified because electrons hopping from one site to its nearest neighbors would suffer phase shifts according to the AB effect.[22] Selection of these phase shifts is arbitrary as long as it ensures that electrons circling a plaquette once suffer a phase shift $\delta$ ($\delta = 2\pi\phi/\phi_0$ as before). In the appendixes, we shall present more discussions on this point. Here, we adopt a symmetric phase configuration, as shown in Fig. 4. Electrons hopping along (against) the arrows suffer a phase shift of $\delta/4(-\delta/4)$. Specifically, one has $t_{ij} = t\exp(i\delta_{ij})$ and

$$\langle ij\rangle = (0,1),\ (0,-1),\ (1,0),\ (-1,0),$$
$$\delta_{ij} = -\delta/4,\ -\delta/4,\ \delta/4,\ \delta/4. \tag{21}$$

Thus the mean-field Hamiltonian in $k$ space is

$$H = \sum_{k\sigma}\left[\left(\frac{Un}{2} + Um\sigma\right)c_{k\sigma}^{+}c_{k\sigma} + \left(\frac{Un}{2} - Um\sigma\right)d_{k\sigma}^{+}d_{k\sigma}\right] - \sum_{k\sigma}(\gamma_k c_{k\sigma}^{+}d_{k\sigma} + \mathrm{H.c.}), \tag{22}$$

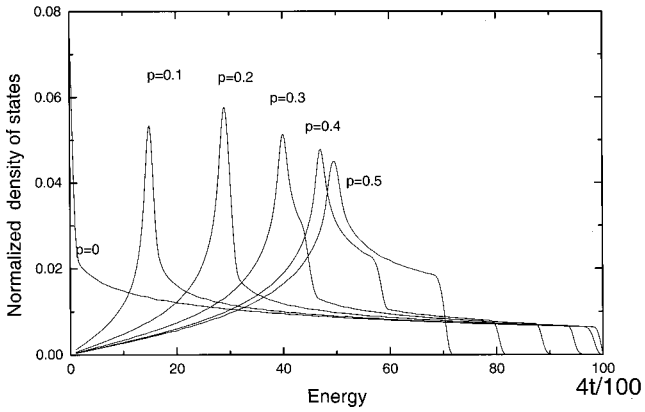


FIG. 5. Normalized density of states versus energy for different magnetic fluxes, where $p=\phi/\phi_0$ and $m=0$. The curves are symmetric with respect to $\phi=0.5\phi_0$, i.e., the curve for $p$ which is less than 0.5 is exactly identical to that for $1-p$.

where

$$\gamma_k = 2te^{i\delta/4}\cos k_x a + 2te^{-i\delta/4}\cos k_y a, \tag{23}$$

and the energy spectrum is

$$\epsilon_k^{\pm} = \frac{Un}{2} \pm \sqrt{|\gamma_k|^2 + (Um)^2}$$

$$= \frac{Un}{2} \pm 2t[\cos^2 k_x a + \cos^2 k_y a + 2\cos k_x a \cos k_y a \times \cos\delta/2 + (Um/2t)^2]^{1/2}. \tag{24}$$

The antiferromagnetic order parameter $m$ is determined by the following self-consistent equation:

$$1 = \frac{U}{N}\sum_k \frac{f(\epsilon_k^-) - f(\epsilon_k^+)}{\sqrt{|\gamma_k|^2 + (Um)^2}}. \tag{25}$$

For the half filled case, the lower subband is completely filled while the upper subband is empty. When the staggered magnetic flux is zero, the Fermi surface is nested: $k_x \pm k_y = \pm\pi$. However, as one turns on the staggered magnetic flux, the Fermi surface consists of four points: $(\pm\pi/2, \pm\pi/2)$. The original square Fermi surface has been concave inside, which is illustrated in Fig. 5 by the shifted peaks of the density of states as $p=\phi/\phi_0$ varies. Because of this property, the singularity in Eq. (25) is, however, very different from the situation without magnetic flux ($\phi=0$) and the integral or the sum of Eq. (25) always converges. Thus there exists a nonzero critical value $U_c$ for the onset of the antiferromagnetic order

$$U_c = \left(\frac{1}{N}\sum_k |\gamma_k|^{-1}\right)^{-1}, \tag{26}$$

and we show its dependence on magnetic flux $\phi$ in Fig. 6. This is similar to the case of introducing next-nearest-neighbor hoppings,[30,31] although their mechanisms are different. Here, the nonzero $U_c$ is caused by the magnetic flux and it can be changed as one tunes the magnetic flux. Thus we

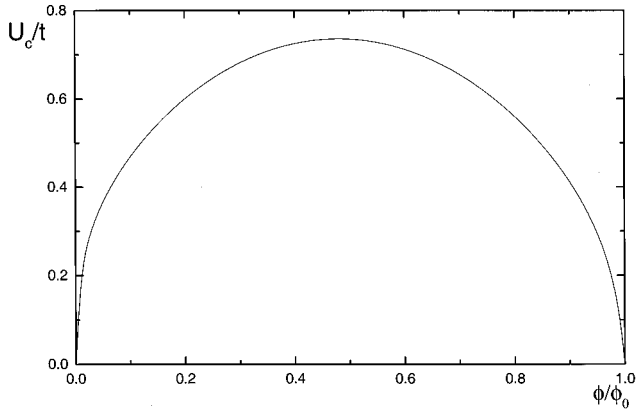


FIG. 6. The critical value $U_c/t$ versus magnetic flux $\phi/\phi_0$. The curve is symmetric with respect to $\phi=0.5\phi_0$, and periodic with period $\phi_0$.

have proved the statement that the existence of staggered magnetic flux suppress the occurrence of antiferromagnetic ordering. In fact, in the large $U$ limit, we have

$$m = \frac{1}{2} - 4\frac{t^2}{U^2} + 3(1+\cos^2\delta)\frac{t^4}{U^4}, \tag{27}$$

and it can be seen that finite $\delta$ decreases $m$. Now we can achieve a magnetic-field-induced metal-insulator transition by modulating $\phi$ if $U$ is less than $U_c^{\max}\sim 0.735t$. This transition happens because antiferromagnetic order would disappear in a certain region of $\phi$ [where $U_c(\phi)>U$] and the system changes from an insulator [where $U_c(\phi)<U$] into a metal.

The bandwidth $W$ and the band gap $\Delta$ are

$$W = 2t\sqrt{2(1+|\cos\delta/2|) + (Um/2t)^2} - Um, \tag{28}$$

$$\Delta = 2Um. \tag{29}$$

Once more, one sees that both $W$ and $m$ (hence the band gap $\Delta$) are functions of $\phi$ with period $\phi_0$, while the energy spectrum $\epsilon_k$ is with period $2\phi_0$. This should be an intrinsic property, regardless of dimensionality. From Fig. 5, it can be seen that the bandwidth is a decreasing function of $\phi$ with $\phi$ ranging from 0 to $0.5\phi_0$. This means that the effective electron hopping would be suppressed by increasing the staggered magnetic flux within that region.

When antiferromagnetic order is absent, $m=0$, a ''$d$-wave-type'' pseudogap would be opened on the original Fermi surface, $\cos k_x + \cos k_y = 0$,

$$\tilde{\Delta} = \tilde{\Delta}_0 |\cos k_x - \cos k_y|, \tag{30}$$

where

$$\tilde{\Delta}_0 = 2\sqrt{2}t\sqrt{1-|\cos\delta/2|}. \tag{31}$$

The density of states near the Fermi surface is

$$\rho(\varepsilon) = \frac{\pi}{|\sin\delta/2|t^2}|\varepsilon| \quad \text{when} \quad |\varepsilon| \ll t|\sin\delta/2|. \tag{32}$$

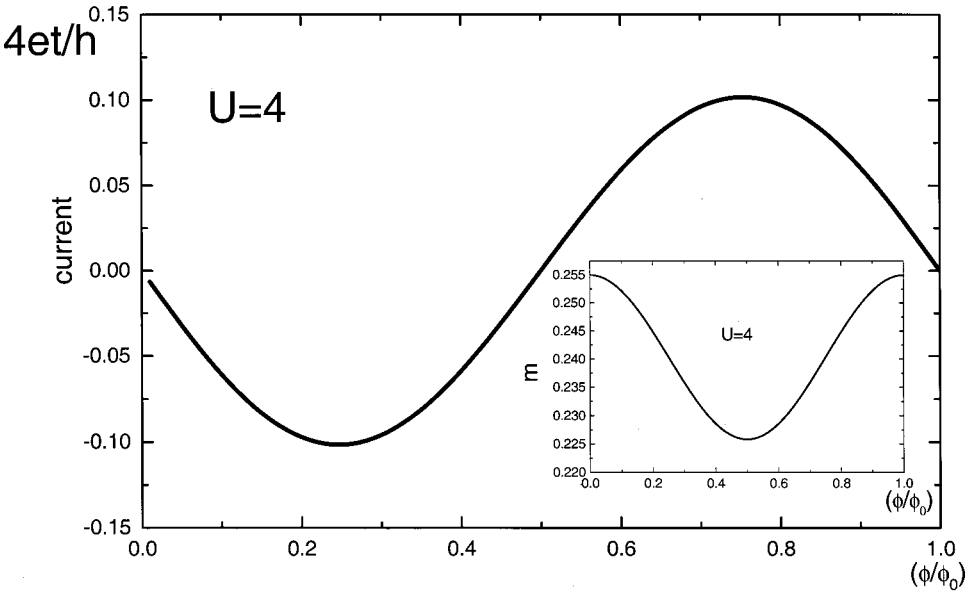


FIG. 7. Induced currents versus magnetic flux $\phi/\phi_0$ for $U=4t$. The inset shows the flux dependence of sublattice magnetization $m$.

As a comparison, we give the density of states for the normal state with $\phi=0$

$$[\rho_N(\varepsilon)\propto\ln|\varepsilon| \quad \text{when} \quad |\varepsilon|\ll t|]. \tag{33}$$

The power-law behavior of $\rho(\varepsilon)$ will be reflected in most thermodynamical properties of the system.

For comparison to the quasi-one-dimensional case, we also investigate the flux dependence of the field-induced current of the system. Explicitly, let us consider the current in the $x$ direction. Straightforward evaluation gives

$$\begin{aligned} I_x &= \frac{2et}{\hbar}\mathrm{Im}(e^{i\delta/4}\langle c^+_{i+a}d_i\rangle) \\ &= \frac{4et}{N\hbar}\sum_k \mathrm{Im}(e^{ik_x a+i\delta/4}\langle c^+_{k\sigma}d_{k\sigma}\rangle) \\ &= \frac{4et}{h}\sin(\delta/2)A(\delta), \end{aligned} \tag{34}$$

where

$$A(\delta)=\frac{1}{2\pi}\int_{k\in BZ} dk\cos(k_x a)\cos(k_y a)/\sqrt{|\gamma_k|^2+(Um)^2}. \tag{35}$$

The flux dependences of the current is shown in Fig. 7. As before, the induced current is a function of $\phi$ with period $\phi_0$. The induced current exhibits no oscillation behavior as we observed for the quasi-one-dimensional case when flux $\phi$ is modulated through $\frac{1}{2}\phi_0$. Instead, it changes smoothly through zero. In a similar manner, one obtains the current flowing in other directions,

$$I_{-x}=-I_y=-I_{-y}=I_x. \tag{36}$$

Using the translational invariance, one can get the distribution of the induced current of the whole system. The distribution is exactly the same as that shown by the arrows in Fig. 4. The only difference is that in a period of $\phi_0$, the direction of the induced current changes twice.

Now let us discuss the stability of the current distribution. With staggered magnetic fluxes introduced, persistent current will occur in the system. The total magnetic flux does not come merely from the external field, for there exists additional magnetic fluxes produced by the induced current. The distribution of these self-induced magnetic fluxes can deviate from the perfect staggered distribution. In Appendix A, we have studied this fluctuation effect in detail and have come to the conclusion that the staggered magnetic-flux state or the symmetric current state is stable under fluctuation.

Since the perfect staggered magnetic-flux state is stable, it is interesting to know what will happen if by any chance there is a fluctuation to the flux configuration shown in Fig. 4. Such fluctuation could come from disorder in the hopping integral, destruction of antiferromagnetic background due to the motion of electrons, etc. To start, we discuss the case corresponding to the magnetic-flux configuration as shown in Fig. 8(b):

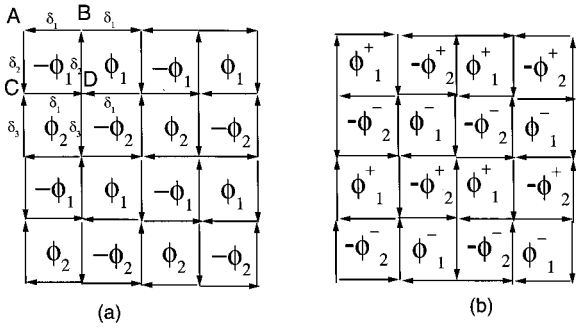


FIG. 8. A symmetric deviation to the staggered magnetic field is made in the system. A, B, C, and D are the four types of sites in the corresponding sublattices, and $\delta_1$ and $\delta_2$ are the phase shifts of electrons hopping along the arrows.

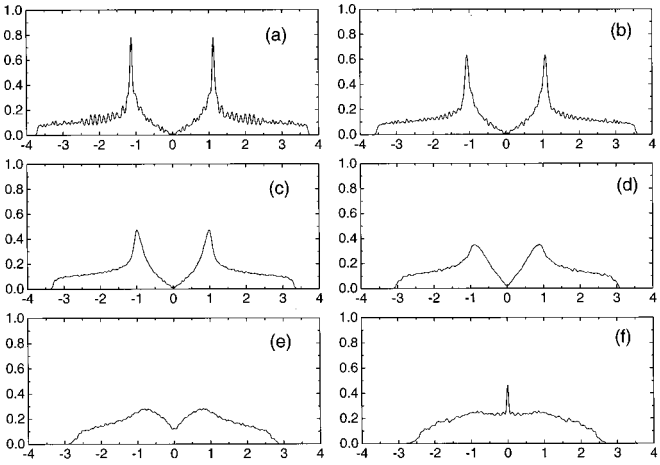


FIG. 9. Density of states for various values of disorder strength for the same staggered magnetic field with $\phi=0.2\phi_0$ and (a) $\delta\phi=0.2\phi_0$; (b) $\delta\phi=0.4\phi_0$; (c) $\delta\phi=0.6\phi_0$; (d) $\delta\phi=0.8\phi_0$; (e) $\delta\phi=1.0\phi_0$; and (f) $\delta\phi=1.2\phi_0$.

$$\phi_1^{\pm}=\phi\pm\delta\phi_1,\quad \phi_2^{\pm}=\phi\pm\delta\phi_2, \tag{37}$$

where $\delta\phi_{1(2)}$ are small fluctuations. For this configuration, we have calculated energy dispersion and found that zero gaps occur at the following 16 points:

$$\left(\pm\frac{\pi}{2}\pm w(-),\quad \pm\frac{\pi}{2}\pm w(+)\right), \tag{38}$$

where

$$w(\pm)=\frac{\pi}{2\phi_0}(\delta\phi_1\pm\delta\phi_2). \tag{39}$$

Thus, compared with the case of perfect staggered magnetic flux, Eq. (30), the number of points on the Fermi surface with zero gap is quadrupled. For the configuration shown in Fig. 8(a) which is a special case of Fig. 8(b) with $\delta\phi_1=\delta\phi_2$, the number of points with zero gap is just doubled. So we expect to have finite density of states with zero gap on the Fermi surface as the fluctuation in magnetic flux becomes strong. To investigate this problem, we introduce randomness into the magnetic flux $\phi$ such that

$$\phi_i=(-1)^{i_x+i_y}\phi_0+\delta\phi*\mathrm{RAND}[-1,\ 1], \tag{40}$$

where RAND$[-1, 1]$ stands for random numbers uniformly distributed over $-1$ and 1. For random $\phi_i$, an analytical solution is impossible so we diagonalize the Hamiltonian matrix numerically for a $40\times40$ site lattice as an illustration. In Fig. 9, we present results of the density of states (DOS) for $\phi_0=0.2$, $\delta\phi/\phi_0=0.2$, 0.4, 0.6, 0.8, 1.0, and 1.2. Some wiggles appearing in Fig. 9 are just finite-size effects. Here we assume that there is no antiferromagnetic ordering, i.e., $\Delta=0$. We observe that as $\delta\phi$ is increased: (i) the system has more and more states with zero gap, i.e., the Fermi surface has evolved from several points to a finite region around points $(\pm\pi/2,\ \pm\pi/2)$, consistent with the conclusion we draw for Fig. 8(b). Since the states in the center of the energy band are delocalized, i.e., extended,[6,7] the conductivity would increase continuously with the fluctuation of the staggered magnetic field. (ii) When $\delta\phi$ is large enough, the DOS resembles that for the tight-binding model in the absence of the staggered magnetic field because the singularity of the DOS at zero energy was recovered gradually. Similar calculations for $\phi=0$ have also been performed and the singularity at zero energy are still present. This feature is in agreement with previous results.[6,32] (iii) The bandwidth is a decreasing function of $\delta\phi$. This means that the effective electron hopping can be suppressed by the fluctuation of the staggered magnetic field.

## IV. SUMMARY

In summary, we have investigated magnetic-field-induced metal-insulator transition by studying the tight-binding and the Hubbard models with hopping integral modulated by magnetic flux in one and two dimensions. In one dimension, the one-band model with uniform as well as alternating magnetic flux and the two-band model are considered and compared with each other. We showed that a magnetic-field-induced metal-insulator transition can be achieved. The bandwidth, the energy gap, and the conductance were calculated and we showed that they are all periodic functions of $\phi$ with period $\phi_0$. Such periodic behavior is also true in two dimensions so it is an intrinsic property, regardless of dimensionality. For the two-dimensional case, we found that the staggered magnetic flux suppresses antiferromagnetic ordering. Peaks in the density of states are shifted by the magnetic flux. The magnetic-field-induced metal-insulator transitions can also be realized. The introduction of staggered magnetic flux opens an anisotropic *d*-wave pseudogap at the Fermi surface. Thus most thermodynamical properties of the half filled system should follow power laws at low temperatures. The distribution of induced current was analyzed. It satisfies the conservation law and exhibits no anomalies. The stability of the distribution of induced current was discussed and we found that the symmetric current distribution is stable. We also studied the effect of different phase configurations and found that they have no effect on the physical properties of the system (see the Appendixes for more details), as expected. Finally, we introduced fluctuations into magnetic flux and studied its effects on the density of states. We showed that the system developed a finite portion of Fermi surface with zero gap around four points $(\pm\pi/2,\ \pm\pi/2)$, whereas for the perfect staggered magnetic-flux case, these four points are the only points on the Fermi surface with zero gap. Thus the conductivity of the half filled band would increase with the fluctuation. The bandwidth is a decreasing function of the fluctuation.

## ACKNOWLEDGMENTS

We wish to acknowledge financial support from the Research Grants Council (RGC) of the Hong Kong Special Administrative Region under project CUHK 4190/97P and the Chinese Nature Science Foundation.

## APPENDIX A

In this appendix, the stability of the staggered magnetic-flux state or the symmetric current state is studied. To address this question, let us consider other distributions which have small deviations from the staggered one shown in Fig. 4. We treat these deviations as perturbations and see what will happen. For simplicity, we consider the case of small $U$ ($U<U_c$) so that $m=0$. For physical consideration, let us discuss the case shown in Fig. 8(a), where a symmetric deviation is made. With $\phi_1=\phi-\delta\phi$ and $\phi_2=\phi+\delta\phi$, the reduced Hamiltonian is given by (we set the lattice constant to be 1 here)

$$H=-t\sum_k\ (2e^{-i\delta_1}\cos k_x B_k^+ A_k+(e^{i\delta_3+ik_y}+e^{i\delta_2-ik_y})C_k^+ A_k +(e^{-i\delta_3+ik_y}+e^{-i\delta_2-ik_y})D_k^+ B_k+2e^{i\delta_1}\cos k_x D_k^+ C_k +\text{H.c.}), \tag{A1}$$

where $A_k/B_k/C_k/D_k$ refer to annihilation operators at sites $A/B/C/D$ and

$$\delta_1=\frac{\pi}{2}\phi/\phi_0,\quad \delta_2=\delta_1-\frac{\pi\delta\phi}{\phi_0}=\delta_1-y,\quad \delta_3=\delta_1+y, \tag{A2}$$

with $y=\pi\delta\phi/\phi_0$ being a small quantity. The equation that determines the energy spectrum is

$$\det\begin{Bmatrix}\omega & -a & -c^* & 0\\ -a^* & \omega & 0 & -b\\ -c & 0 & \omega & -a^*\\ 0 & -b^* & -a & \omega\end{Bmatrix}=0, \tag{A3}$$

where

$$a=2te^{i\delta_1}\cos k_x,\quad b=2te^{i\delta_1}\cos(k_y+y),$$
$$c=2te^{i\delta_1}\cos(k_y-y). \tag{A4}$$

The energy spectrum is

$$\omega_k=\pm[\tfrac{1}{2}((2|a|^2+|b|^2+|c|^2)\pm\{(2|a|^2+|b|^2+|c|^2)^2 -4[|a|^4+|b|^2|c|^2-2\,\mathrm{Re}(a^2bc)]\}^{1/2})]^{1/2}. \tag{A5}$$

The ground state of the system is the state with the two lower subbands filled and the two higher subbands left completely empty. After tedious calculations, we get the ground-state energy of the system,

$$E=E_0+\eta y^2, \tag{A6}$$

where $E_0$ is the ground-state energy of the unperturbed system and

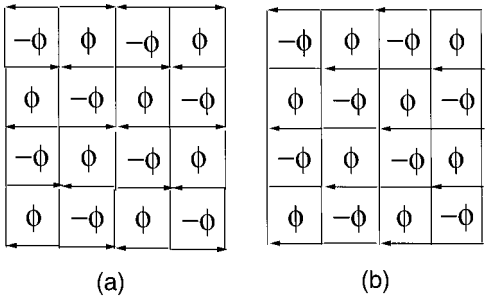


FIG. 10. Another two kinds of distribution of phase shift. Electrons hopping along arrows suffer a phase shift: (a) $\delta/2$, and (b) $\delta$. These configurations ensure that any electron circling a plaquette suffers a phase shift $\delta$.

$$\eta=\frac{2t^2\sin^2\delta/2}{|\cos\delta/2|}\sum_k\frac{|\cos k_y|}{|\cos k_x|}\left(\frac{1}{\sqrt{|a|^2+|d|^2-2|a||d||\cos\delta/2|}} -\frac{1}{\sqrt{|a|^2+|d|^2+2|a||d||\cos\delta/2|}}\right), \tag{A7}$$

with $d=2te^{i\delta_1}\cos k_y$. Obviously, $\eta>0$ so $E_0$ is the minimum energy of the ground state, i.e., the distribution of the current discussed is stable.

## APPENDIX B

In this appendix, we address the question of whether the distribution of current and other properties depend on the selection of phase configurations or not. The similarity between the distribution of current and the symmetric phase configuration should be a coincidence, because the selection of phase configurations can be quite arbitrary and the current distribution should be independent of it. In the following discussions, we shall consider two other different phase configurations and come to the same conclusion: the different selection of phase configurations has no effect on the physical properties of the system.

First we choose one kind of phase configuration as shown in Fig. 10(a), where electrons hopping along (against) the arrows suffer a phase shift $\delta/2$ ($-\delta/2$). Obviously, this distribution satisfies the requirement that electrons circling around an ''atom cell'' once would suffer a phase shift $\delta$. The system could also be described by the Hamiltonian Eq. (22) with $\gamma_k$ substituted by $\gamma_k'$,

$$\gamma_k'=te^{i\delta/2}\cos k_x a+t\cos k_y a. \tag{B1}$$

Because $|\gamma_k'|$ is exactly identical to $|\gamma_k|$, the energy spectrum in this case is identical to the former, Eq. (24). So thermodynamic quantities certainly do not change. Considering the current in the $x$ direction, one has

$$I_x=\frac{2et}{\hbar}\,\mathrm{Im}\,e^{i\delta/2}\langle c_{i+x}^+ d_i\rangle, \tag{B2}$$

and it is exactly the same as before. After some manipulations, one gets the same result as Eq. (34). Hence the distribution of the current is still shown by the arrows in Fig. 4.

Now let us consider another kind of phase configuration shown in Fig. 10(b), where electrons hopping along (against) the arrows suffer a phase shift $\delta$. Similar to the above case, the system could also be described the Hamiltonian Eq. (22) with $\gamma_k$ substituted by $\gamma_k''$,

$$\gamma_k'' = t(e^{ik_x a} + e^{-ik_x a + i\delta}) + 2t\cos k_y a. \tag{B3}$$

The corresponding energy spectrum is

$$\omega_k = \frac{Un}{2} \pm \sqrt{|\gamma_k''|^2 + (Um)^2}$$

$$= \frac{Un}{2} \pm 2t[\cos^2(k_x a - \delta/2) + \cos^2 k_y a + 2\cos(k_x a - \delta/2)\cos k_y a \cos\delta/2 + (Um/2t)^2]^{1/2}. \tag{B4}$$

The energy spectrum looks different from Eq. (24), but the only difference is that the wave vector of the former has been uniformly shifted by $(\delta/2, 0)$, relative to the latter. The partition function $Z$ does not change, because $Z$ is a sum over the whole $k$ space in the Brillouin zone. Thus thermodynamic quantities do not change, either. Similar to the above case, the current in the $x$ direction is

$$I_x = \frac{2et}{\hbar}\mathrm{Im}\langle c_{i+x}^{+} d_i\rangle. \tag{B5}$$

Straightforward calculation gives

$$I_x = \frac{et}{N^2\hbar}\sin\delta/2 \sum_k \cos(k_x a - \delta/2)\cos k_y a \frac{f_F(|\gamma_k''|) - f_F(-|\gamma_k''|)}{|\phi_k''|}$$

$$= \frac{4et}{h}\sin(\delta/2)A(\delta). \tag{B6}$$

The current $I_x$ is identical to the result of Eq. (34), so the current distribution does not change, either.

One can choose any other different phase configuration and then obtain different Hamiltonians and dispersion relations but with the same result: all the differences are superficial and have no effect on the physical properties of the system. The different phase configurations just correspond to the different magnetic vector potential for the same magnetic field. As a matter of fact, this is nothing but the consequence of gauge invariance.[33]

*Corresponding author. Electronic address: hqlin@phy.cuhk.edu.hk


[1] R. B. Laughlin, Phys. Rev. B **23**, 5632 (1981); B. I. Halperin, *ibid.* **25**, 2185 (1982).
[2] B. I. Halperin, Patrik A. Lee, and Nicholas Read, Phys. Rev. B **47**, 7312 (1993).
[3] K. Chahra, T. Ohono, M. Kasai, Y. Kanke, and Y. Kozono, Appl. Phys. Lett. **62**, 780 (1993).
[4] R. von Helmolt, J. Wecker, B. Holzapfel, L. Schultz, and K. Samwer, Phys. Rev. Lett. **71**, 2331 (1993).
[5] K. Yang and R. N. Bhatt, Phys. Rev. B **55**, 1922 (1997).
[6] Akira Furusaki, Phys. Rev. Lett. **82**, 604 (1999).
[7] D. N. Sheng and Z. Y. Weng, Phys. Rev. Lett. **75**, 2388 (1995).
[8] X. C. Xie, X. R. Wang, and D. Z. Liu, Phys. Rev. Lett. **80**, 3563 (1998).
[9] S. V. Kravchenko, D. Simonian, M. P. Sarachik, Whitney Mason, and J. E. Furneaux, Phys. Rev. Lett. **77**, 4938 (1996).
[10] Dragana Popović, A. B. Fowler, and S. Washburn, Phys. Rev. Lett. **79**, 1543 (1997).
[11] S. N. Evangelou, Phys. Rev. Lett. **75**, 2550 (1995).
[12] T. Sugiyama and N. Nagaosa, Phys. Rev. Lett. **70**, 1980 (1993).
[13] A. G. Aronov, A. D. Mirlin, and P. Wölfle, Phys. Rev. B **49**, 16 609 (1994).
[14] Derek K. K. Lee and J. T. Callker, Phys. Rev. Lett. **72**, 1510 (1994); Derek K. K. Lee, J. T. Callker, and D. Y. K. Ko, Phys. Rev. B **50**, 5272 (1994).
[15] Y. B. Kim, A. Furusaki, and Derek K. K. Lee, Phys. Rev. B **52**, 16 646 (1995).
[16] K. Yakubo and Y. Goto, Phys. Rev. B **54**, 13 432 (1996).
[17] R. Ugajin, J. Appl. Phys. **76**, 2833 (1994); R. Ugajin, Phys. Rev. B **53**, 10 141 (1996).
[18] V. Dobrosavljević, E. Abrahams, E. Miranda, and Sudip Chakravarty, Phys. Rev. Lett. **79**, 455 (1997).
[19] Daisuke Takai and Kuniichi Ohta, Phys. Rev. B **50**, 2685 (1994); **50**, 18 250 (1994).
[20] Zhiwen Pan, Shijie Xiong, and C. D. Gong, Phys. Rev. E **58**, 2408 (1998); Zhiwen Pan, C. D. Gong, M. H. Lung, and H. Q. Lin, *ibid.* **59**, 6010 (1999).
[21] H. L. Mak, H. Q. Lin, and C. D. Gong, J. Appl. Phys. **87**, 30 (2000).
[22] Y. Aharonov and D. Bohm, Phys. Rev. **115**, 485 (1959).
[23] E. Abrahams, P. W. Anderson, D. C. Licciardello, and V. Ramakrishnan, Phys. Rev. Lett. **42**, 673 (1979).
[24] P. A. Lee and T. V. Ramakrishnan, Rev. Mod. Phys. **57**, 287 (1985).
[25] M. Büttiker, Y. Imry, and R. Landauer, Phys. Lett. **96A**, 365 (1983); M. Büttiker, Phys. Rev. B **32**, 1846 (1985).
[26] Ho-Fai Cheung, Yuval Gefen, Eberhard K. Reidel, and Wei-Heng Shih, Phys. Rev. B **37**, 6050 (1988).
[27] C. R. Bennett and B. Tanatar, Phys. Rev. B **55**, 7165 (1997).
[28] G. A. Toombs, Phys. Rep. **40c**, 181 (1978).
[29] B. Renker, Phys. Rev. Lett. **30**, 1141 (1973).
[30] J. E. Hirsch, Phys. Rev. B **31**, 4403 (1985).
[31] H. Q. Lin and J. E. Hirsch, Phys. Rev. B **35**, 3359 (1987).
[32] G. Theodorou and M. H. Cohen, Phys. Rev. B **13**, 4597 (1976); T. P. Eggarter and R. Riedinger, *ibid.* **18**, 569 (1978).
[33] Y. R. Wang, Phys. Rev. B **43**, 3786 (1991); **46**, 151 (1992).